1

Hexa-Band Multi-Standard Planar Antenna Design for Wireless Mobile Terminal

Yu-Jen Chi[1] and Chien-Wen Chiu[2]
[1]Department of Electrical Engineering, National Chiao Tung University,
[2]Department of Electric Engineering, National Ilan University,
Taiwan

1. Introduction

Electronic devices such as mobile phones and laptop computers are parts of modern life. Users of portable wireless devices always desire such devices to be of small volume, light weight, and low cost. Thanks to the rapid advances in very large scale integration (VLSI) technology, this dream has become a reality in the past two decades. As technology grows rapidly, a mobile is not just a phone recently. The highly integration of circuits makes the mobile phone and the PDA (personal digital assistant) been combined into a single handset, which is called a smart phone. Also, the Internet carries various information resources and services, such as electronic mail, online chat, file transfer and file sharing, these attractive proprieties make wireless internet service becomes an important function that should be integrated into mobile devices. There are many ways for the user to connect to the internet. The traditional wireless local area network (WLAN) is a popular communication system for accessing the Internet. However, the reach of WiFi is very limited. WLAN connectivity is primarily constrained to hotspots, users need to find the access points and can only use it in certain rooms or areas. As the user get out of range of the hotspot, the signal will become very weak and the user may lose the connection. This disadvantage limits the mobility of wireless communication. Except for the widely used wireless local area network, third generation (3G) mobile telephony based on the High Speed Downlink Packet Access (HSDPA), which is part of the UMTS standards in 3G communications protocol, is another high speed wireless internet access service. It has become popular nowadays that people can get to the internet via cellular communication system. This technology gives the users the ability to access to the Internet wherever the signal is available from the cellular base station. However, the quality sometimes depends on the number of users simultaneously connected per cellular site. In addition to utilizing WLAN/3G dual-mode terminals to enhance efficiency of mobile number portability service, WiMAX (the Worldwide Interoperability for Microwave Access) is an emerging telecommunications technology that provides wireless data transmission in a variety of ways, ranging from point-to-point links to full mobile cellular-type access. WiMAX is similar to Wi-Fi but it can also permit usage at much greater distances. The bandwidth and range of WiMAX make it suitable for the applications like VoIP (Voice over Internet Protocol) or IPTV (Internet Protocol Television). Many people expect WiMAX to emerge as another technology that may be adopted for handset devices in the near future.

The rapid progress in mobile communication requires that many functions and wireless communication systems be integrated into a mobile phone. When portability is taken into account, antenna that can be built in the phone device is desirable. This has led to a great demand for designing multiband antennas for handset devices. Among existing built-in or internal type scheme, the inverted-F (IFA) or planar inverted-F antenna (PIFA) are the most promising candidates. The linear inverted-F antenna, which is the original version of the PIFA, has been described by R. King in 1960 as a shunt-driven inverted-L antenna-transmission line with open-end (king et al., 1960). The PIFA, which is constructed by replacing the linear radiator element of IFA with a planar radiator element, can also be evolved from a microstrip antenna. Taga first investigated PIFA's performance for 800MHz band portable unit radio in 1987 (Taga & Tsunekawa, 1987). He also wrote a chapter in his textbook to teach how to design a single band PIFA (Hirasawa & Haneishi, 1922). The PIFA or IFA are not only small in size but also have a broadband bandwidth. Since it is cheap and easy to fabricate, it has become very popular with mobile phone manufacturers. Many references concerning PIFA and its relatives were published in the decade.

In the past decade, researches for variation of the PIFA and multiband antenna grow rapidly like mushroom. Tri-band, quad-band, penta-band or hexa-band antenna can be found in many journals (Chiu & Lin, 2002; Guo et al., 2003, 2004; Ciais et al., 2004; Chen, 2007; Bancroft, 2005; Ali & Hayes, 2000; Soras et al., 2002; Nepa et al., 2005; Wong et al., 2005; Liu & Gaucher, 2004, 2007; Wang et al., 2007). For example, Chiu presented a tri-band PIFA for GSM800/DCS1800/PCS1900 in 2002 (Chiu & Lin, 2002) . Using two folded arms between the two plates, Guo at el. proposed a compact internal quad-band for covering GSM900/DCS1800/PCS1900 and ISM2450 bands (Guo, et al., 2003). By adding three quarter-wavelength parasitic elements to create new resonances, Ciais et al. presented a design of a compact quad-band PIFA for mobile phones (Ciais et al., 2004). In 2004, Guo & Tan proposed a new compact six-band but complicated internal antenna. His antenna is comprised of a main plate, a ground plane, a parasitic plate and a folded stub perpendicular to the two main plates (Guo & Tan, 2004).

In order to integrate all the wireless services into a mobile terminal and have an effective usage of the precious board space in the mobile device, multiband antenna that is designed to operate on several bands is necessary. However, designing a multiband antenna in a narrow space is a great challenge; a method that decrease the complexity of the antenna structure is also necessary to be investigated. Guo et. al. have recently designed quad-band antennas for mobile phones (Chiu & Lin, 2002; Nashaat et al., 2005; Karkkainen, 2005) and dual-band antennas for WLAN operations (Su & Chou, 2008). However, few of these antennas simultaneously cover the following communication standards: GSM (880-960 MHz), DCS (1710-1880 MHz), PCS (1850-1990 MHz), UMTS2100 (1920-2170 MHz), WLAN + Bluetooth (2400-2480 MHz), WiMAX (2500-2690 MHz), HiperLAN/2 in Europe (5150-5350 / 5470-5725 MHz) and IEEE 802.11a in the U.S. (5150-5350 / 5725-5825 MHz) (Liu & Gaucher, 2004, 2007; Wang et al., 2007; Rao & Geyi, 2009; Nguyen et al., 2009; Anguera et al., 2010; Kumar et al., 2010; Liu et al., 2010; Hsieh et al., 2009; Yu & Tarng, 2009; Hong et at., 2008; Guo et al., 2004; Li et al., 2010). This chapter proposes a planar multiband antenna that comprises a dual-band inverted-F resonator and two parasitic elements to cover all the communication standards mentioned above. One element is devoted to generating a dipole mode and another is helpful to excite a loop mode so as to broaden the impedance bandwidth. This hepta-band antenna is designed for a mobile device and the parasitic element broadens the impedance bandwidth to about 45.5%. This antenna is extended to simultaneously operate in WLAN, WiMAX, and WWAN systems. It covers all cellular bands world-wide and all wireless network bands, such as the following communication standards: GSM/DCS/PCS/UMTS/WLAN/WiMAX/HIPERLAN2/IEEE 802.11. The antenna structure that measures only 50 mm x 12 mm x 0.5 mm can be easily fabricated by stamping from a metal plate. The following describes the details of the proposed antenna as well as the experimental results.

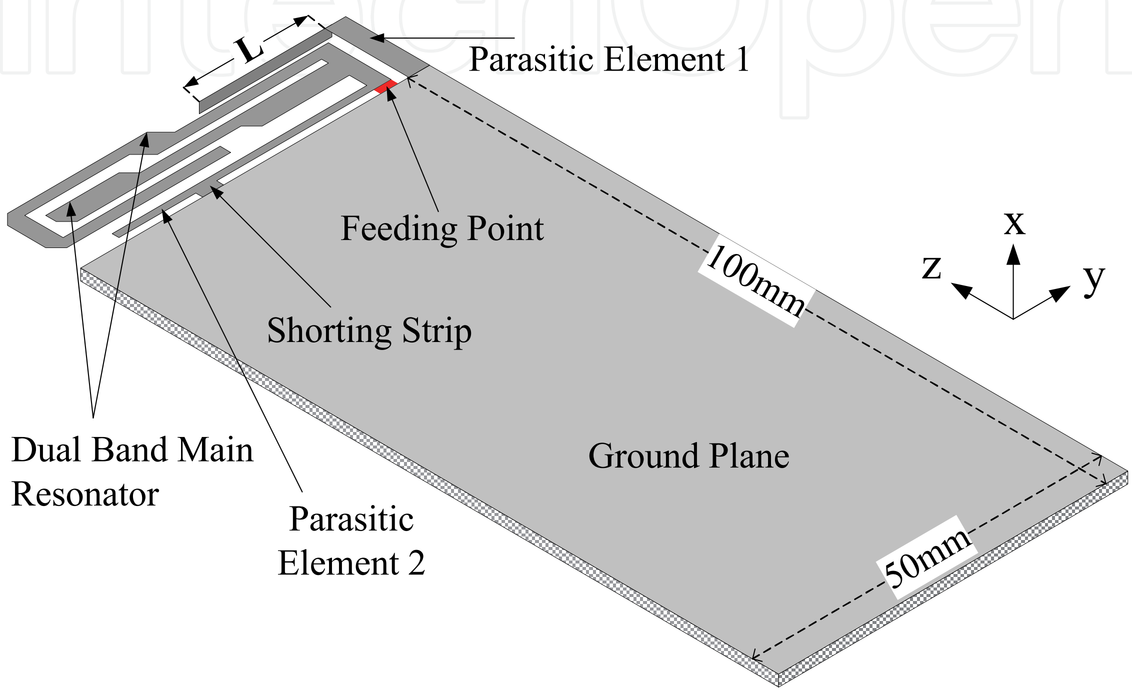

(a)

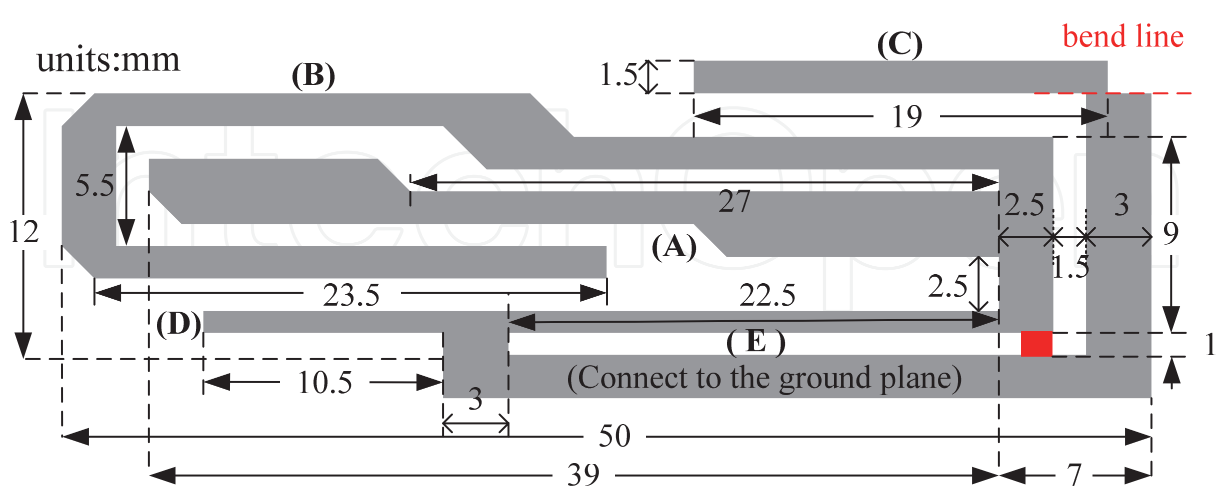

(b)

Fig. 1. The proposed antenna (a) Three-dimensional configuration of the proposed antenna (b) Plane view of the antenna structure.

2 Antenna design

2.1 Design of a dual-band antenna

Modern mobile terminals require small and thin design, therefore, planar inverted-F antenna, which requires a spacing of about 7 mm ~ 12 mm between the antenna and the substrate to achieve the sufficient operating bandwidth, is not suitable to be integrated with the present thin mobile terminals although it is popular and widely used. Fig. 1(a) shows a three dimensional view of the proposed design. The antenna, which is mounted on the top edge of the printed circuit board (PCB), is fed by a 50 Ω coaxial cable. The antenna is coplanar with the system ground of the PCB. The dielectric constant of the PCB used here is 4.4 and the thickness is 1.58 mm. As shown in Fig. 1(b), this radiating structure measures 50 mm × 12 mm × 1.5 mm and can be extended to a single metallic plate. It is basically an inverted-F antenna in which the quarter-wavelength characteristic is obtained thanks to a short-circuited metallic strip. As indicated in Fig. 1(b), this design comprises a direct-feed dual band main resonator with two branches (A) and (B), and two parasitic elements (C) and (D) excited by electromagnetic coupling, to achieve multiband operation.

Shown in Fig. 2 is a typical configuration of an inverted-F antenna. It can be fed by a mini-coaxial cable which is connected to the RF module. Here, H is the height of the radiator above the ground plane, L_F is the horizontal length from the feed point to the open end of the antenna, and L_B is the horizontal length from the feed point to the closed end of the antenna. This antenna is a quarter-wavelength radiator with one short end and one open end. The resonant frequency can be easily calculated by the formula:

$$f = \frac{c}{4(H + L_B + L_F)}$$

the where *c* is the speed of light. The resonant frequency can be adjusted by changing the value L_F, and the distance L_B between the feed point and shorting strip can be used to adjust the input impedance. The height H of the antenna is closely related to the impedance bandwidth where the Q factor can be reduced by increasing the antenna height to broaden the bandwidth and vice versa. Variations of IFA Antenna height cause some effects on bandwidth. Fig. 3 shows the simulation results with different antenna height H. It is found that increasing the height will increase the impedance bandwidth.

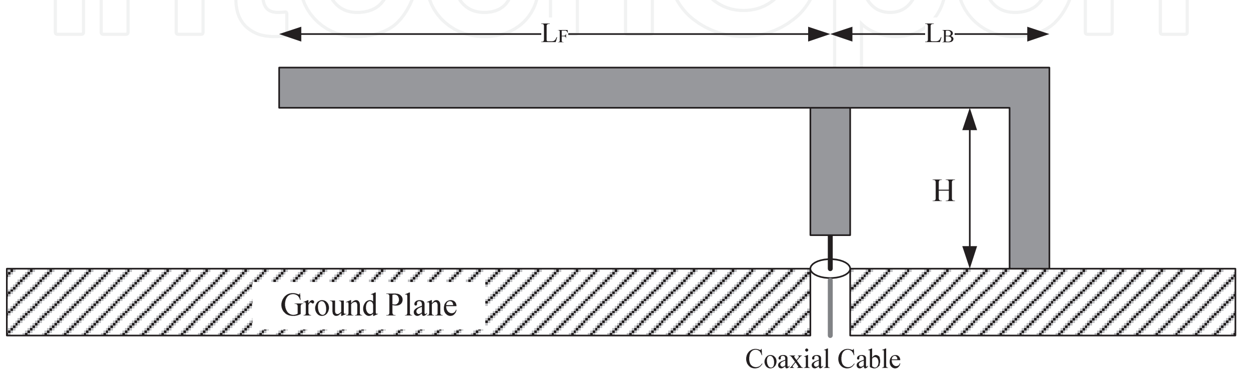

Fig. 2. A typical inverted-F Antenna.

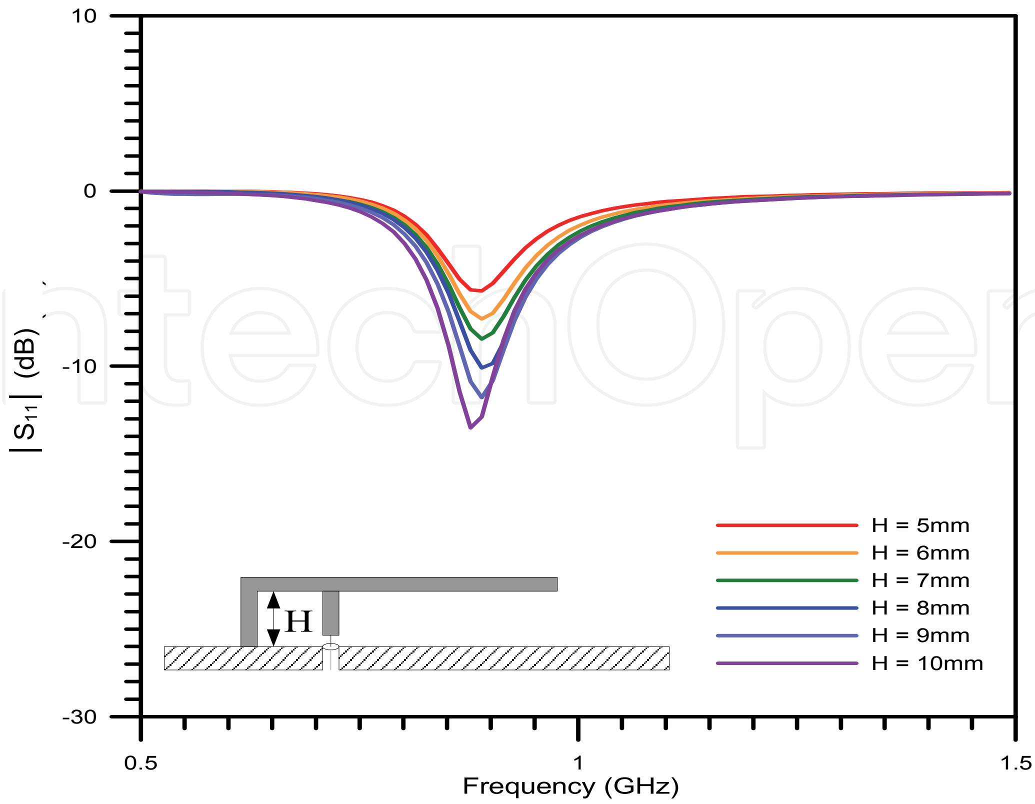

Fig. 3. Antenna height influences on the impedance bandwidth for a simple IFA.

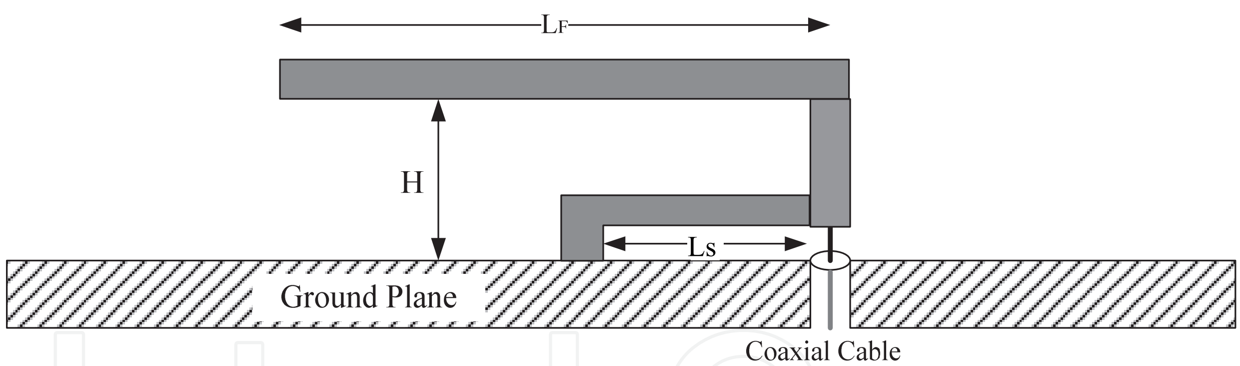

Fig. 4. A variation of typical inverted-F antenna.

Fig. 4 shows another kind of inverted-F antenna while the shorting pin is moved to the bottom for size reduction. The mechanism of this alternative is the same as the previous one, but the input impedance is matched by adjusting the length of the shorting strip L_S.

The dual band inverted-F antenna can be simply accomplished by creating two resonant paths of the antenna element. As shown in Fig. 5, the dual-band main resonator consists of two branches (A and B). The length of the longer branch (B) is about 83 mm (9 + 44.5 + 6 + 23.5 mm) which is one-quarter of the wavelength at 900MHz. The lower resonant mode for GSM operation can be excited on this resonator. On the other hand, branch (A) in the middle creates a shorter path of 42 mm, which is about a quarter of wavelength at 1800 MHz. As a result, the resonant mode for DCS operation can be excited. Simulation result of the dual band antenna is shown in Fig. 6. The input impedance can be adjusted by changing the length of the shorting strip L_s . In this case, L_s is selected to be 22.5 mm to have the widest bandwidth at both lower and upper band.

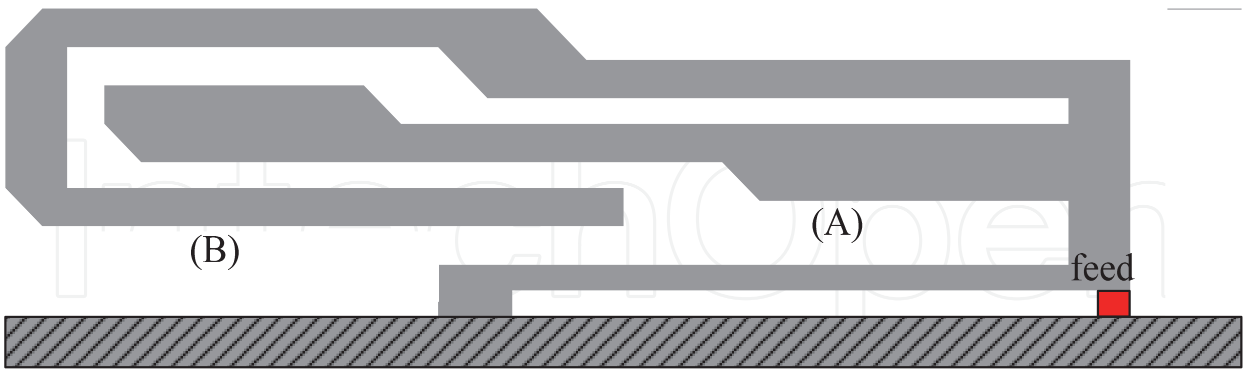

Fig. 5. A dual band inverted-F main resonator.

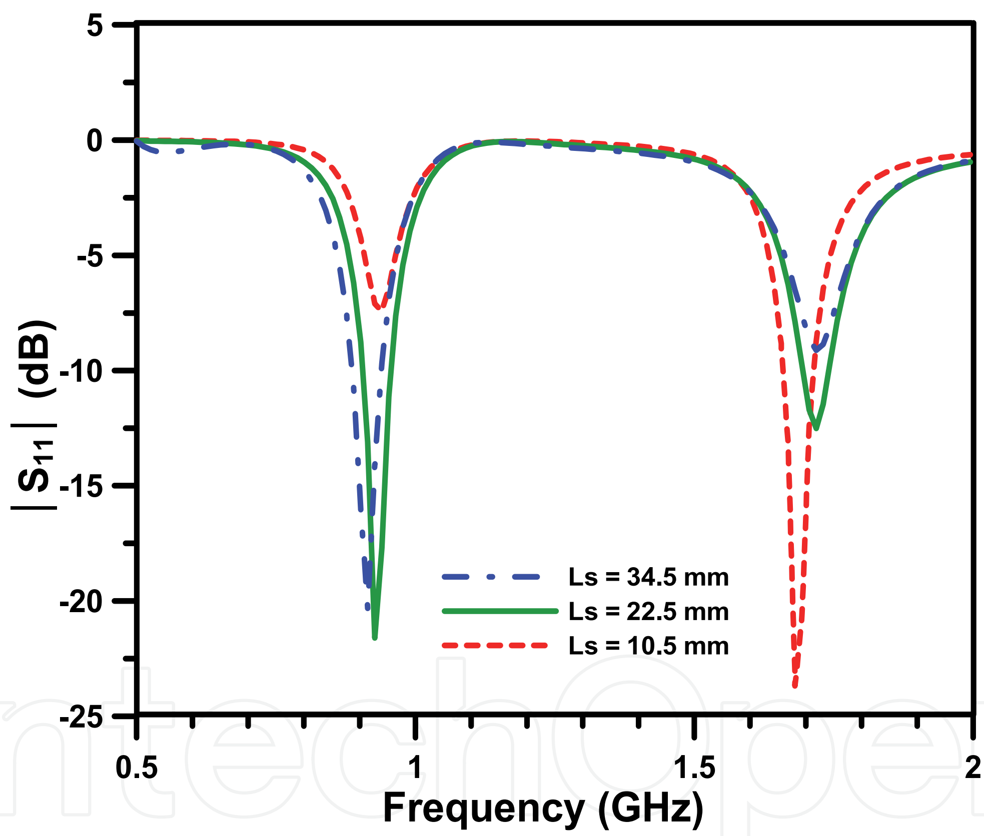

Fig. 6. Parameter study with different value of Ls.

2.2 Bandwidth enhanced by a parasitic element

Creating multiple resonant paths of the inverted-F antenna is helpful to generate multiple resonances. However, the coupling between each resonant path makes it difficult to match the antenna at each frequency band. To cover the wide bandwidth from 1900 MHz to 2700 MHz, this work introduces a parasitic resonator C near the main driven resonator. This parasitic element is excited by electromagnetic coupling from the main dual band resonator. Thus, a dipole-like antenna that resonates at 2250 MHz is formed by both the introduced resonator C, and the main resonators A and B. Fig. 7 shows the surface current distributions on the resonators and the ground plane. Finding show that part of the dual band resonator and the parasitic element form a dipole antenna. From point a, through point b, c, and d, then to point f in Fig. 7, the total length (39 mm + 3 mm + 9 mm + 19 mm = 70 mm) is closed to 0.5 wavelength at 2250MHz (67 mm). This allows the antenna to generate an additional 0.5-wavelength resonant mode at 2250 MHz to cover the desired operation bands.

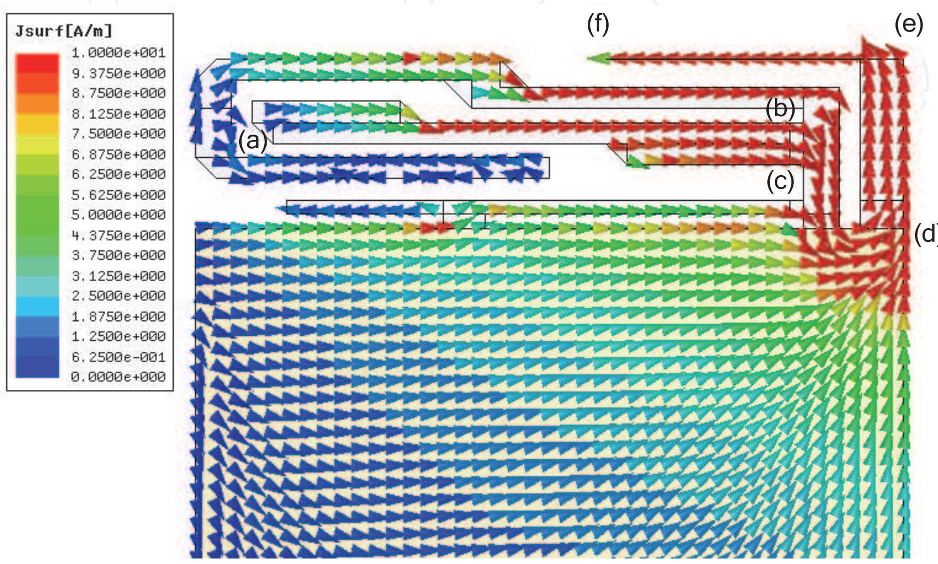

Fig. 7. Victor surface current distribution at 2.25 GHz.

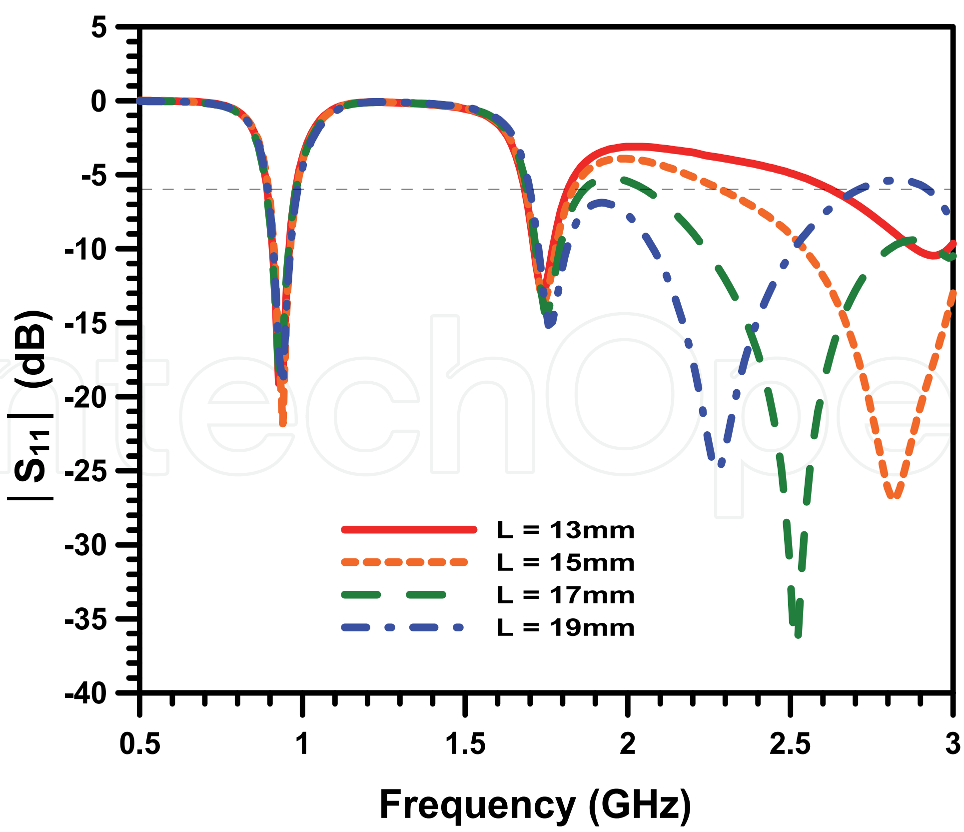

Fig. 8. Parameter study with different length of the parasitic resonator.

To demonstrate the effect of the parasitic element covering from 1900 MHz to 2700 MHz, Fig. 8 shows the parameter study of the proposed antennas with different length of the parasitic element. By Investigating the Smith chart shown in Fig. 9, it is evident that the input impedance is closer to 50 Ω as length L increases, because the longer the parasitic element, the more the loaded capacitance (Chi, 2009). The narrow gap between the main resonator and the parasitic element C introduces a proper capacitance to compensate for possible inductance contributed from the dual-band main resonator. Increasing capacitance neutralizes the effect due to inductance of the strip. Therefore, the capacitive coupled parasitic element creates a new resonant mode but does not change the original two resonant modes at 900 MHz and 1800 MHz. The length of the parasitic element is selected to be 19 mm to have the return loss better than 6 dB in the band of operation. The achieve bandwidth of the parasitic element is about 34.78 %, covering from 1900 MHz to 2700 MHz, which is enough for WLAN, WMAN, and WWAN operations.

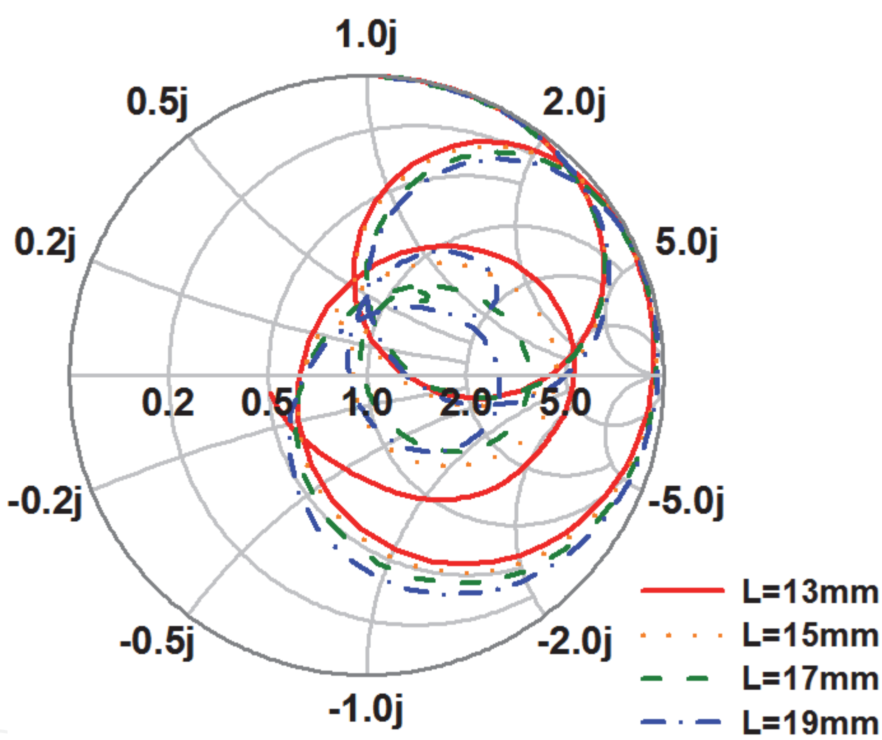

Fig. 9. Parametric study – Smith Chart.

2.3 Create resonances at the U-NII band

So far, a hexa-band Inverted-F antenna has been designed, except IEEE 802.11a or HYPERLAN/2. The current research will include the U-NII (Unlicensed National Information Infrastructure) band in this design by a tuning parasitic resonator D, as Fig. 1(b) shows. First, the third harmonics of the resonating frequency in the second band (1.72 GHz) is about 5.20 GHz. This mode which contributes to the U-NII band is also excited. The surface current distribution on the resonator A in Fig. 10(a) demonstrates that the 1.5 wavelength mode generates at the resonating frequency. The vector current distribution is shown in Fig. 11(a). Second, the loop resonator E in Fig. 1(b) is designed as a one-wavelength rectangular loop antenna. The perimeter of the loop antenna (25.5 mm + 1 mm +

25.5 mm + 1 mm) is roughly equal to a wavelength of the resonant frequency 5.59 GHz (53.67 mm). Fig. 10 (b) shows surface current distributions at the resonating frequency 5.59 GHz, The vector current distribution shown in Fig. 11(b) demonstrates that one-wavelength loop mode is excited on the resonator E.

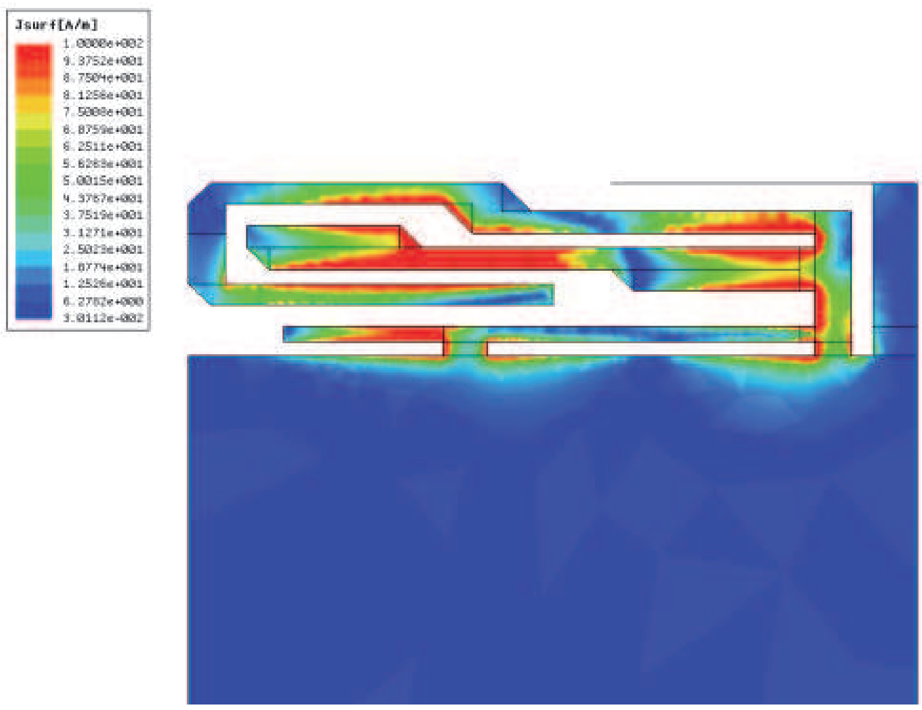

(a)

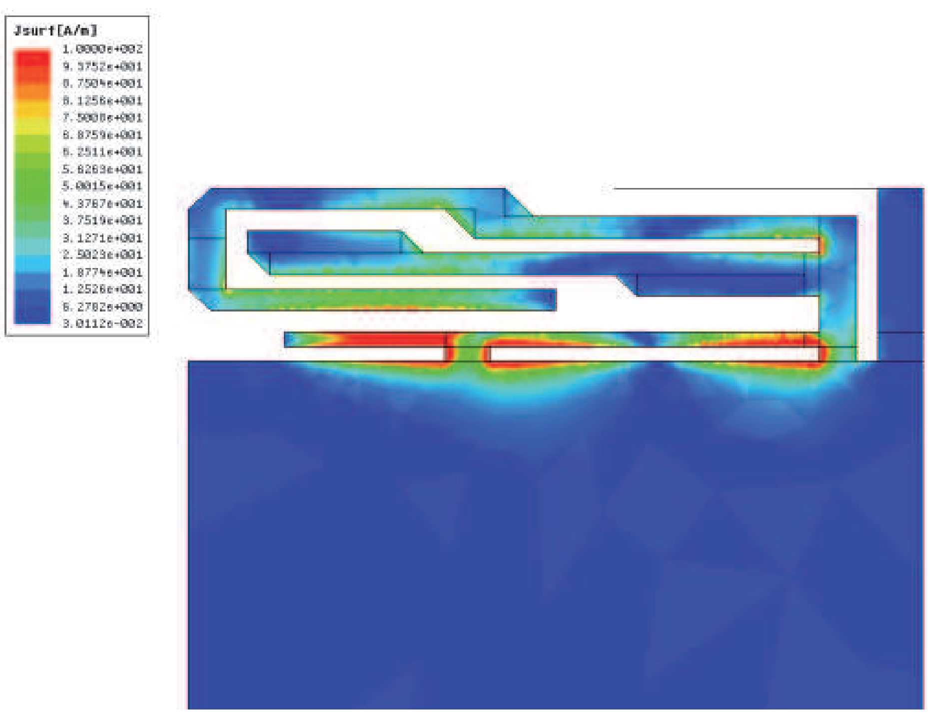

(b)

Fig. 10. Surface current distribution at (a) 5.20 and (b) 5.59 GHz.

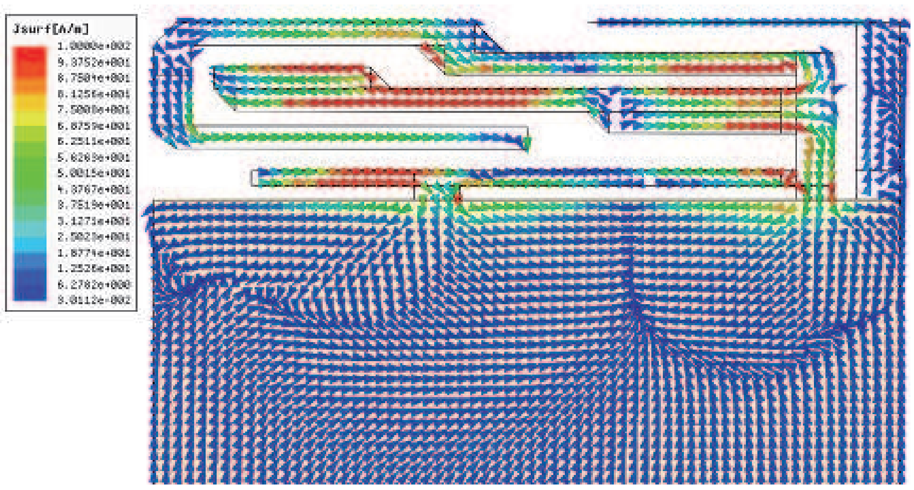

(a)

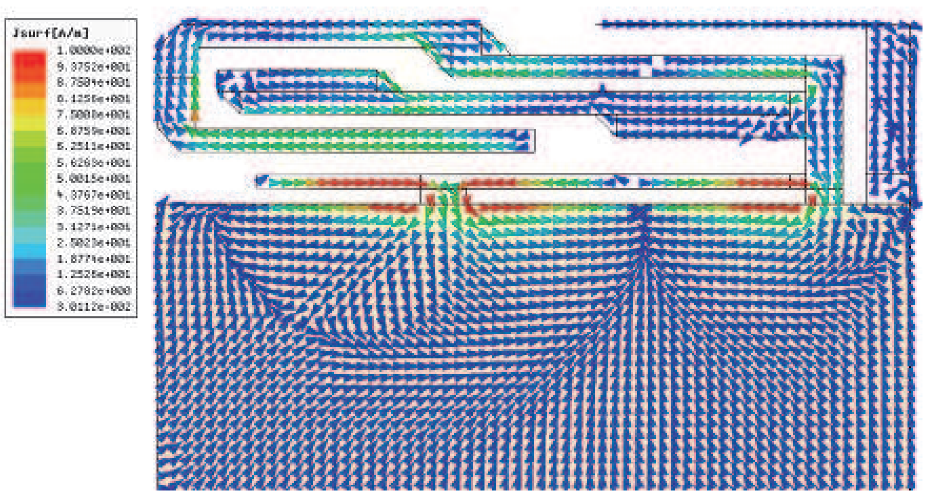

(b)

Fig. 11. Victor current distributions at higher U-NII bands: (a) 5.20 and (b) 5.59 GHz.

Finally, this work applies another technique to tune the higher order resonances for the U-NII band. The quarter wavelength resonating at 6.0 GHz is only about 12.5 mm. A short resonator D with a length of 10.5 mm, as Fig. 1(b) shows, is introduced to the short-circuited pin of the main resonator to form an inverted L-shape parasitic element. The capacitive coupling between the strip and the chassis increases its electrical length since the radiating strip is only 1 mm above the ground plane. Adding this parasitic element improves resonance performance at the U-NII band.

3. Results and discussion

This study constructs and tests the proposed antenna based on the design dimensions shown in Fig. 1(b). The test structure was shown in Fig. 12 and the measurement of scattering parameters was performed by an Agilent E5071B network analyzer. Fig. 13 shows the measured and simulated return loss where the solid red line is the measured result and the dotted blue line is the simulated one. Findings show good agreement between the measured data and simulated results. The antenna covers all cellular bands used world-wide is evident. The achieved bandwidths with return loss better than 6 dB are 80 MHz (880–960 MHz) in the GSM band, 1000 MHz (1700–2700 MHz) in the DCS/PCS/UMTS/WiFi /WiMAX band and 1270 MHz (4820–6090 MHz) in the 5 GHz U-NII band. When ground plane length varies from 80 mm to 120 mm, frequency shifting is slight (Chi, 2009).

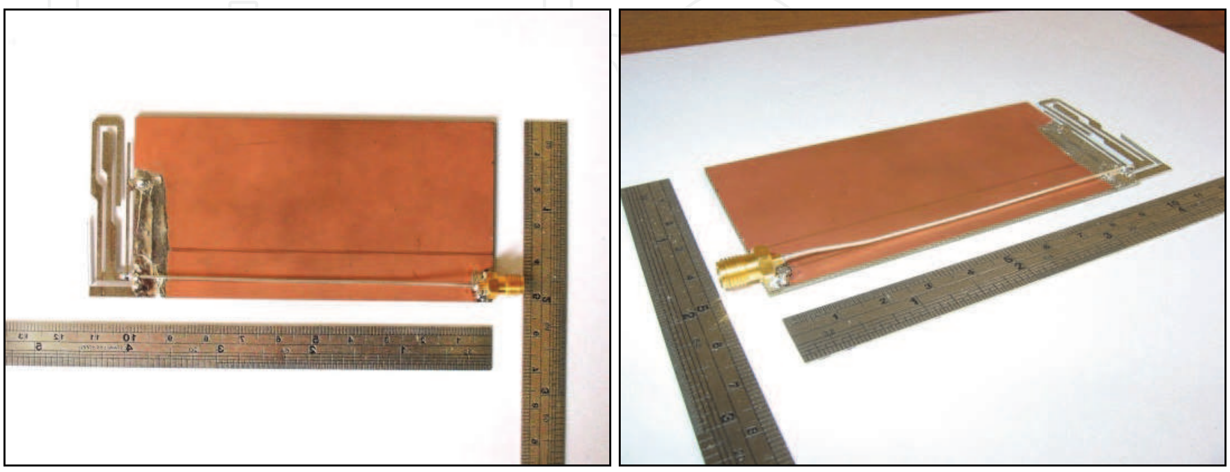

(a) (b)

Fig. 12. Photography of the fabricated antenna (a) top view, (b) side view.

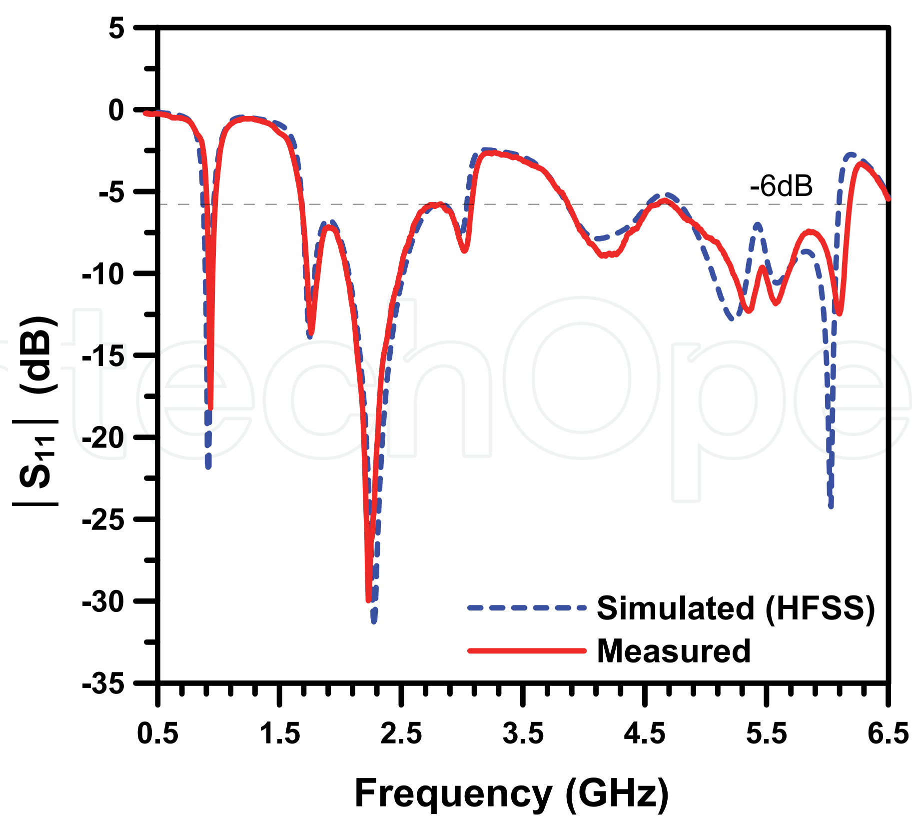

Fig. 13. Measured and simulated results of the proposed antenna.

This study performed radiation-pattern and gain measurement in the anechoic chambers of SGS Ltd. Taiwan, as shown in Fig. 14. Fig. 15 shows the measured and simulated radiation patterns at the xy-cut, xz-cut, and yz-cut. The measured radiation patterns show a good match to the simulation results except at 925MHz. In the small antenna measurement, the patterns are easily affected by the feeding RF cable in the GSM band (Chen et al., 2005). This work finds that the dual-polarization radiation-patterns have very suitable characteristics for portable devices. For the radiation shown in Fig. 14(a), more energy for E_θ is radiated in the lower band as compared to $E\varphi$. The $E\varphi$ field has some dips at 900 MHz on the xz-plane or 1800 MHz on the xy-plane. This is probably due to current cancellation on the strips and the ground plane.

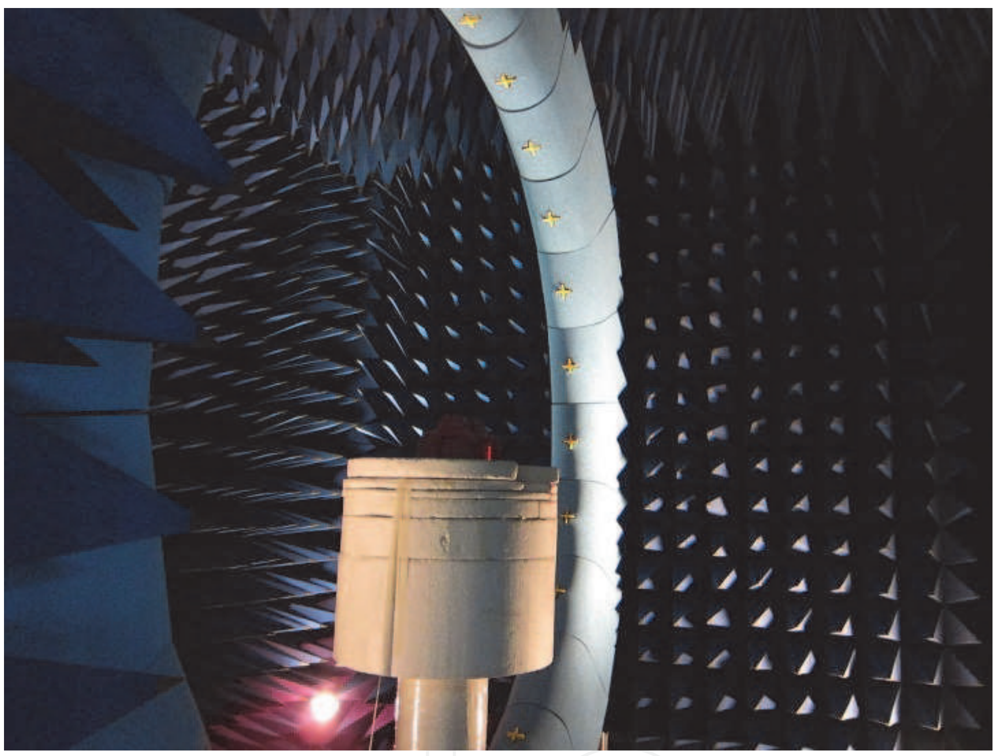

Fig. 14. Radiation Pattern measurement in a 3D anechoic chamber.

Findings also show a dipole-like pattern at the frequency 2170 MHz. Radiation patterns shown in Fig. 15(b) confirm this deduction. The radiation pattern of this mode is similar to a small dipole oriented in the y–axis leading to a directional pattern in the E-plane (xy-plane, blue line) and omni-directional pattern in the H-plane (xz-plane, blue line), as Fig. 15(b), shows respectively. The resonators C and B at 2170 MHz have strong current distributions along the z-direction which also contribute to radiation fields. The radiation pattern of this current distribution is due to a small dipole oriented in the z–axis leading to a bidirectional pattern in the E-plane (xz-plane, red line) and omni-directional pattern in the H-plane (xy-plane, red line), as Fig. 15(b), shows respectively. Findings also show an asymmetric radiation pattern at the U-NII band (5-6 GHz) and some variation and nulls, since different modes are excited in this U-NII band.

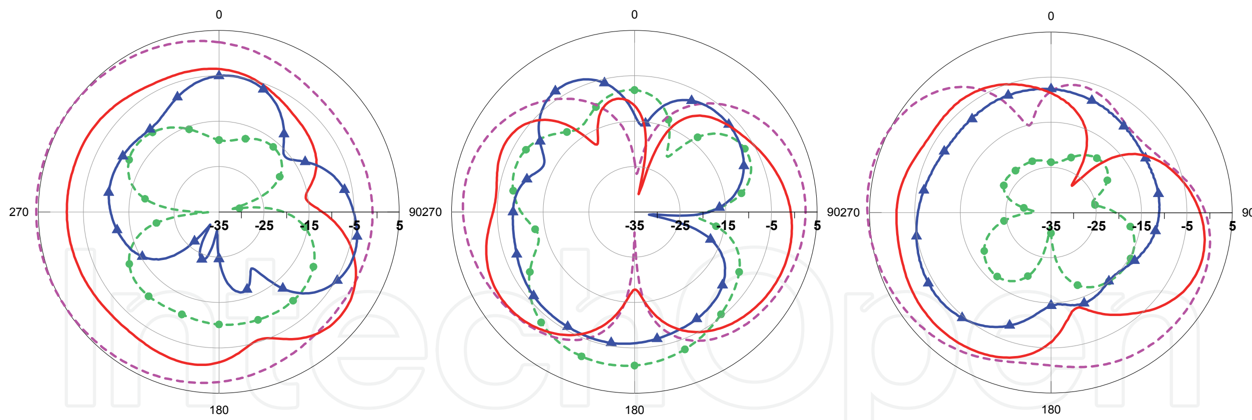

x-y plane x-z plane y-z plane

(a) 925 MHz

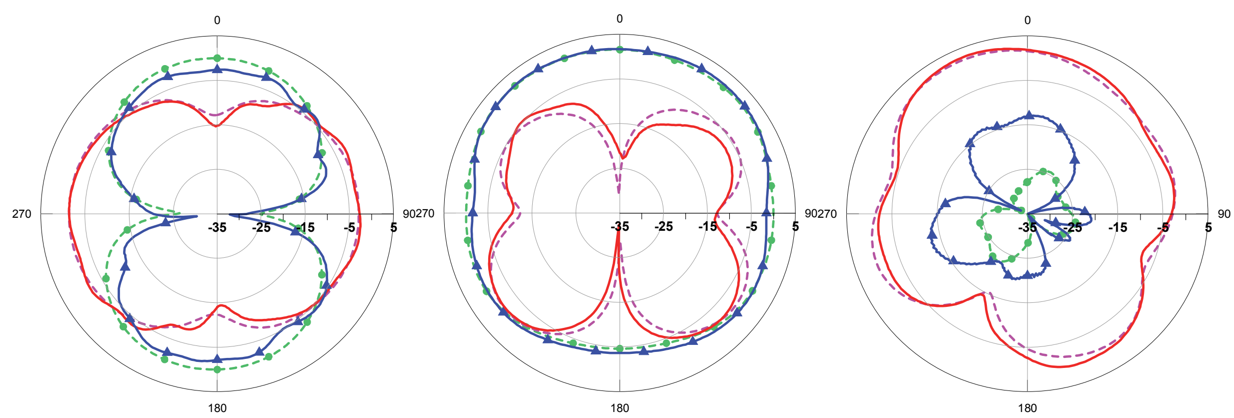

x-y plane x-z plane y-z plane

(b) 2170 MHz

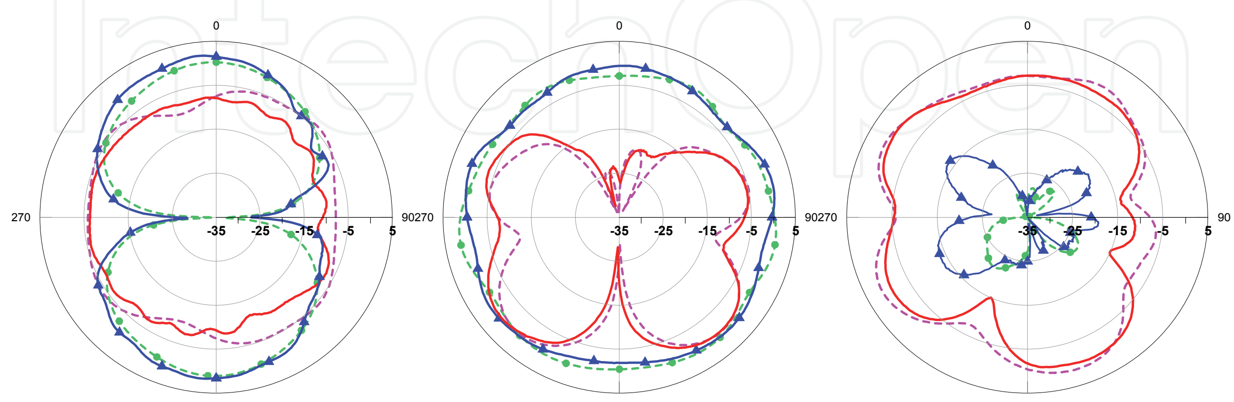

x-y plane x-z plane y-z plane

(c) 2650 MHz

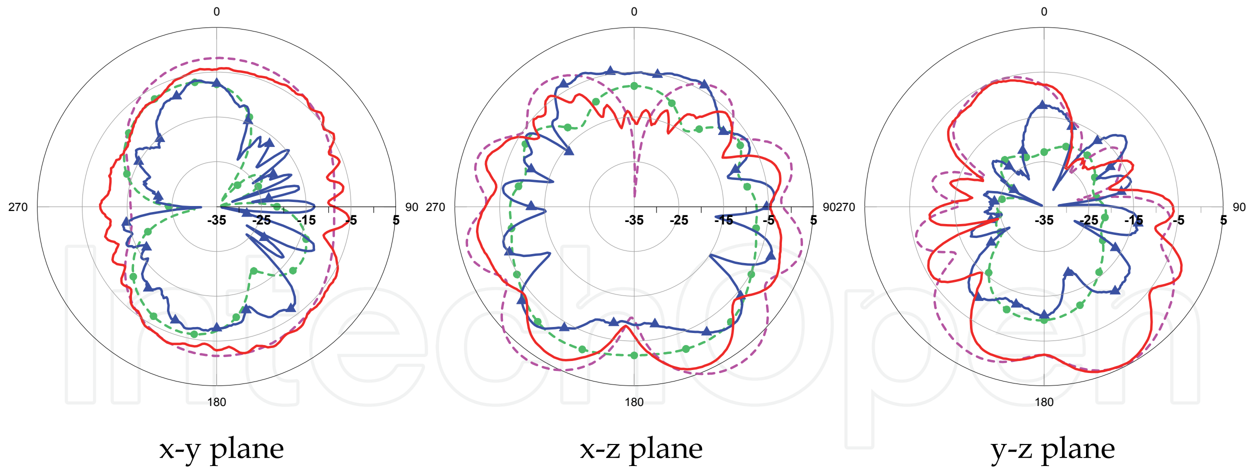

(d) 5775 MHz

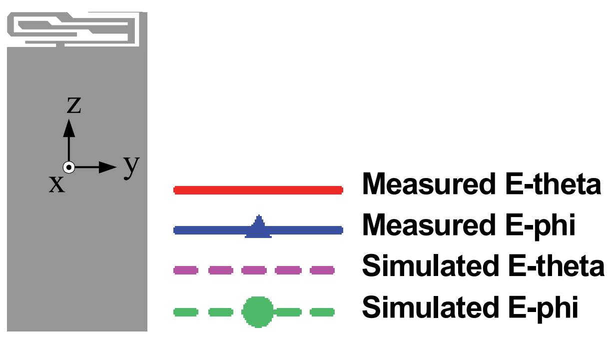

Fig. 15. Measured and simulated radiation patterns in three cuts (a) 925 MHz (b) 2170 MHz (c) 2650 MHz (d) 5775 MHz.

Frequency (MHz)	925	1710	1795	1920	1990
Peak Gain (dBi)	-0.25	2.4	2.05	1.39	1.63
Average Gain (dBi)	-1.96	1.10	-0.63	-0.01	-0.51
Efficiency	51.42%	61.94%	64.85%	70.35%	78.80%
Frequency	2170	2420	2650	5250	5800
Peak Gain	2.95	2.5	2.48	6.91	8.35
Average Gain	1.10	1.15	0.58	-0.31	-1.99
Efficiency	90.11%	86.83%	71.42%	70.24%	71.80%

Table 1. Measured three-dimensional peak gain, average gain, and radiation efficiency.

By using the commercial electromagnetic simulation software HFSS, this research carries out simulations for the theoretical gains to investigate antenna performance and compare it with the measured results (Chi, 2009). Good agreement confirms that the measured data are accurate. The two-dimensional average gain is determined from pattern measurements made in the horizontal (azimuth) plane for both polarizations of the electric field. The results are then averaged over azimuth angles and normalized with respect to an ideal isotropic radiator (Chen, 2007). Finally, Table 1 lists the measured peak gain, two-dimensional average gain and radiation efficiency for all the operation bands, showing that all radiation efficiencies are over 50 percent, meeting the specification requirement.

4. Summary

This chapter reported a down-sized multiband inverted-F antenna to integrate the 3.5G and WLAN/WiMAX antenna systems. It is comprised of a dual-band antenna with one feed point and two parasitic elements to cover many mobile communication systems including GSM900 /DCS /PCS /UMTS /WLAN/ WiMAX /HiperLAN2 /IEEE802.11a. Measured parameters including return loss, radiation patterns, three-dimensional peak gain and average gain as well as radiation efficiency were presented to validate the proposed design. Since this antenna can be formed by a single plate, it is both low cost and easy to fabricate, making it suitable for any palm-sized mobile device applications.

5. References

C. Soras, M. Karaboikis, and G. T. V. Makios, "Analysis and design of an inverted-F antenna printed on a PCMCIA card for the 2.4 GHz ISM band," IEEE Antenna's and propagation magazine, vol. 44, no. 1, February 2002.

C. W. Chiu and F. L. Lin, "Compact dual-band PIFA with multi-resonators," Electronics Letters, vol. 38, pp. 538-540, June 2002.

C.-L. Liu, Y.-F. Lin, C.-M. Liang, S.-C. Pan, and H.-M. Chen, "Miniature Internal Penta-Band Monopole Antenna for Mobile Phones," IEEE Trans. Antennas Propag., vol. 58, no. 3, March 2010.

D. Liu and B. Gaucher, "A new multiband antenna for WLAN/Cellular application," Vehicular Technology Conference, vol. 1, 60th, pp. 243 - 246, Sept. 2004.

D. Liu and B. Gaucher, "A quadband antenna for laptop application," International Workshop on Antenna Technology, pp. 128-131, March 2007.

D.M. Nashaat, H. A. Elsadek, and H. Ghali, “Single feed compact quad -band PIFA antenna for wireless communication applications,” IEEE Trans. Antennas Propagat., vol. 53, No. 8, pp. 2631-2635, Aug. 2005.

H.-W. Hsieh, Y.-C. Lee, K.-K. Tiong, and J.-S. Sun, "Design of A Multiband Antenna for Mobile Handset Operations," IEEE Antennas Wireless Propag. Lett., vol. 8, 2009.

J. Anguera, I. Sanz, J. Mumbrú, and C. Puente, "Multiband Handset Antenna with A Parallel Excitation of PIFA and Slot Radiators," IEEE Trans. Antennas Propag., vol. 58, no. 2, February 2010.

K. Hirasawa and M. Haneishi, "Analysis, design and measurement of small and low profile antennas," ch.5, Norwood, MA, Artech House, 1922.

K.-L. Wong, L.-C. Chou, and C.-M. Su, "Dual-band flat-plate antenna with a shorted parasitic element for laptop applications," IEEE Transactions on Antennas and Propagation, vol. 53, no. 1, pp. 539-544, January 2005.

M. Ali and G. J. Hayes, "Analysis of intergated inverted-F antennas for bluetooth applications," IEEE International symposium on antenna and propagation, 2000.

M. K. Karkkainen, “Meandered multiband PIFA with coplanar parasitic patches,” IEEE Microw. Wireless Compon. Lett., vol.15, pp. 630-632, Oct. 2005.

P. Ciais, R. Staraj, G. Kossiavas, and C. Luxey, "Design of an internal quad-band antenna for mobile phones," IEEE Microwave and wireless components letters, vol. 14, no. 4, April 2004.
P. Kumar.m, S. Kumar, R. Jyoti, V. Reddy, and P. Rao1, "Novel Structural Design for Compact and Broadband Patch Antenna," 2010 International Workshop on Antenna Technology (iWAT), 1-3 March 2010.
P.Nepa, G. Manara, A. A. Serra, and G. Nenna, "Multiband PIFA for WLAN mobile terminals," IEEE antenna and wireless propagation letters, vol. 4, 2005.
Q. Rao and W. Geyi, "Compact Multiband Antenna for Handheld Devices," IEEE Trans. Antennas Propag., vol. 57, no. 10, October 2009.
R. Bancroft, "Development and integration of a commercially viable 802.11a/b/g HiperLan/ WLAN antenna into laptop computers," Antennas and Propagation Society International Symposium, vol. 4A, pp. 231- 234, July 2005.
R. King, C. W. Harisson, and D. H. Denton, "Transmission-line missile antenna," IRE Trans. Antenna Propagation, vol. 8, no. 1, pp. 88-90, 1960.
S. Hong, W. Kim, H. Park, S. Kahng, and J. Choi, "Design of An Internal Multiresonant Monopole Antenna for GSM900/DCS1800/US-PCS/S-DMB Operation," IEEE Trans. Antennas Propag., vol. 56, no. 5, May 2008.
S.W. Su and J.H. Chou, "Internal 3G and WLAN/WiMAX antennas integrated in palm-sized mobile devices," Microw. Opt. Technol. Lett., vol. 50, no. 1, pp. 29-31, Jan. 2008.
T. K. Nguyen, B. Kim, H. Choo, and I. Park, "Multiband dual Spiral Stripline-Loaded Monopole Antenna," IEEE Antennas Wireless Propag. Lett., vol. 8, 2009.
T. Taga and K. Tsunekawa, "Performance analysis pf a built-in planar inverted-F antenna for 800MHz and portable radio units," IEEE Trans. on selected areas in communications, vol. SAC-5, no. 5, June 1987.
W. X. Li, X. Liu, and S. Li, "Design of A Broadband and Multiband Planar Inverted-F Antenna," 2010 International Conference on Communications and Mobile Computing, vol. 2, 12-14 April 2010.
X. Wang, W. Chen, and Z. Feng, "Multiband antenna with parasitic branches for laptop applications," Electronics letters, vol. 43, no. 19, 13th, September 2007.
Y. J., Chi, "Design of internal multiband antennas for portable devices," Master Thesis, National Ilan University, June 2009
Y.-C. Yu and J.-H. Tarng, "A Novel Modified Multiband Planar Inverted-F Antenna," IEEE Antennas Wireless Propag. Lett., vol. 8, 2009.
Y.-X. Guo and H. S. Tan, "New compact six-band internal antenna," IEEE antenna and wireless propagation letters, vol. 3, 2004.
Y.-X. Guo, I. Ang, and M. Y. W. Chia, "Compact internal multiband antennas for mobile handsets," IEEE antenna and wireless propogation letters, vol. 2, 2003.
Y.-X. Guo, M. Y. W. Chia, and Z. N. Chen, "Miniature Built-In Multiband Antennas for Mobile Handsets," IEEE Trans. Antennas Propag., vol. 52, no. 8, August 2004.
Z. N. Chen, Antennas for Portable Devices, pp.125-126, John Wiley & Sons, Inc. 2007.
Z. N. Chen, N. Yang, Y. X. Guo, and M. Y. W. Chia, "An investigation into measurement of handset antennas," IEEE. Trans. Instrum. Meas., vol. 54, no.3, pp. 1100–1110, June 2005.
Zhi Ning Chen, "Antennas for Portable Devices," John Wiley & Sons, Inc. 2007, ch.4, pp.115-116.

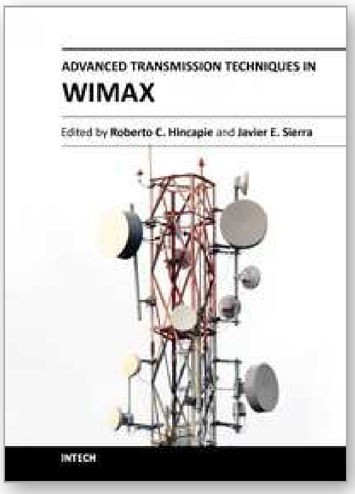

Advanced Transmission Techniques in WiMAX
Edited by Dr. Roberto Hincapie

ISBN 978-953-307-965-3
Hard cover, 336 pages
Publisher InTech
Published online 18, January, 2012
Published in print edition January, 2012

This book has been prepared to present the state of the art on WiMAX Technology. The focus of the book is the physical layer, and it collects the contributions of many important researchers around the world. So many different works on WiMAX show the great worldwide importance of WiMAX as a wireless broadband access technology. This book is intended for readers interested in the transmission process under WiMAX. All chapters include both theoretical and technical information, which provides an in-depth review of the most recent advances in the field, for engineers and researchers, and other readers interested in WiMAX.